

## EVLA OBSERVATIONS OF THE 6035 MHz OH MASERS IN ON 1

VINCENT L. FISH

Jansky Fellow, National Radio Astronomy Observatory, P. O. Box O, 1003 Lopezville Rd., Socorro, NM 87801, vfish@nrao.edu  
*Draft version December 22, 2018*

### ABSTRACT

This Letter reports on initial Expanded Very Large Array (EVLA) observations of the 6035 MHz masers in ON 1. The EVLA data are of good quality, lending confidence in the new receiver system. Nineteen maser features, including six Zeeman pairs, are detected. The overall distribution of 6035 MHz OH masers is similar to that of the 1665 MHz OH masers. The spatial resolution is sufficient to unambiguously determine that the magnetic field is strong ( $\sim -10$  mG) at the location of the blueshifted masers in the north, consistent with Zeeman splitting detected in 13441 MHz OH masers in the same velocity range. Left and right circularly polarized ground-state features dominate in different regions in the north of the source, which may be due to a combination of magnetic field and velocity gradients. The combined distribution of all OH masers toward the south is suggestive of a shock structure of the sort previously seen in W3(OH).

*Subject headings:* masers — ISM: individual (ON 1) — stars: formation — magnetic fields — radio lines: ISM — ISM: molecules

### 1. INTRODUCTION

Onsala 1 (ON 1) is a massive star-forming region with an unusual OH maser spectrum. The ground-state masers, which have been observed interferometrically several times, (e.g., Ho et al. 1983; Argon et al. 2000; Fish et al. 2005a; Nammahachak et al. 2006; Fish & Reid 2007), appear in two disjoint velocity ranges:  $< 6$  km s<sup>-1</sup> and 11–17 km s<sup>-1</sup>, with no maser emission in between. This pattern is reproduced in 6668 MHz methanol emission, which also appears near 0 and 15 km s<sup>-1</sup> (Szymczak et al. 2000).

The masers presently elude clear interpretation. Comparison of OH maser velocities seen in projection against the ultracompact H II region (13–14 km s<sup>-1</sup> after correcting for Zeeman splitting; e.g., from Fish et al. 2005a) with the LSR velocity of the latter derived from a hydrogen recombination line ( $5.1 \pm 2.5$  km s<sup>-1</sup>) led Zheng et al. (1985) to interpret the masers as tracing infall. However, a proper motion study of the OH masers suggests that expansion may dominate the kinematics (Fish & Reid 2007). A more recent model suggests that the OH masers are associated with a molecular outflow (Kumar et al. 2004; Nammahachak et al. 2006). This model proposes a shocked molecular torus origin for the southern masers, but questions remain regarding the overall morphology and velocity structure of the masers in ON 1.

Few northern star-forming regions have been mapped in the 6035 MHz line of OH, in part because few radio arrays in the northern hemisphere have been capable of tuning to the frequency. A previous three-station European VLBI Network (EVN) experiment detected seven 6035 MHz maser features in ON 1 but only observed the redshifted masers (Desmurs & Baudry 1998). Single-dish observations confirm that the 6030 and 6035 MHz masers in ON 1 also appear in two disjoint velocity ranges, but Zeeman pairing ambiguities have prevented a definitive measurement of the magnetic field of the blueshifted masers (Baudry et al. 1997; Fish et al. 2006b).

The upgrade of the National Radio Astronomy Observatory's (NRAO) Very Large Array (VLA) to the Expanded VLA (EVLA) presents new observational opportunities in North America (McKinnon & Perley 2001; Ulvestad et al.

2007). Of interest to spectral line observers is the full frequency coverage between 1 and 50 GHz that will become available. This spring, the EVLA for the first time offered observational capabilities in the extended C-band range of 4.2 to 7.7 GHz, which includes key maser frequencies of OH and methanol. This Letter reports on initial observations of 6035 MHz OH masers with the EVLA.

### 2. OBSERVATIONS

The EVLA was used to observe the 6035.092 MHz line of OH toward ON 1 on 2007 May 25 (experiment code AF459). The array consisted of only the seven telescopes at the time equipped with the first EVLA C-band receivers, since the OH line is outside the tuning range of the older VLA C-band receivers. The antennas used were distributed primarily along the western and northern arms of the VLA A-configuration, giving maximum and minimum baselines of 28.1 and 2.6 km, respectively. Data were taken in both left and right circular polarization (LCP, RCP) using a 781.25 kHz bandwidth divided into 256 spectral channels, providing a channel width of 0.15 km s<sup>-1</sup> and a velocity range of 39 km s<sup>-1</sup> centered at  $v_{\text{LSR}} = 7$  km s<sup>-1</sup> (Doppler tracked). Dual circular correlation products were obtained.

About one hour of usable data were obtained, consisting of 40 minutes on the masers in ON 1 and 10 minutes on the phase calibration source, 2023+318. This was also used to set the flux scale (assuming a flux density of 2.8 Jy from the VLA Calibrator Manual) and for bandpass calibration. Blank sky, single-polarization noise in the image plane with natural weighting was 30 mJy beam<sup>-1</sup> (synthesized beam size  $0''.70 \times 0''.26$ , PA 87°), approximately matching the expected thermal sensitivity. Nevertheless, it is possible that the assumed flux scale is too high by several tens of percent, based on recent variability seen in the flux density of 2023+318 at 4.8 GHz from the VLA flux density history database. The relative uncertainty in the flux scale between the two circular polarizations is better than 10%.

The peak channel of the brightest maser, nearly 50 Jy beam<sup>-1</sup> RCP, was used to determine the absolute position. The location of this maser,  $20^{\text{h}}10^{\text{m}}09^{\text{s}}.090$ ,  $+31^{\circ}31'34''.91 \pm 0''.2$  (J2000), is south and east of the location

obtained from EVN data by Desmurs & Baudry (1998). The data in this channel were iteratively self-calibrated (phase-only and amplitude-and-phase), and calibration solutions were applied to both polarizations in the entire data set. Images measuring  $30''$  in each direction centered on the brightest maser were created in LCP and RCP.

### 3. RESULTS

#### 3.1. Maser Locations

A total of 19 maser features are detected, as listed in Table 1. Two-dimensional Gaussian components were fitted to each patch of maser emission above  $10\sigma$  and grouped into features in one or more adjacent channels. One-dimensional Gaussian components were fitted to the spectrum of each feature to determine the peak flux density and full width at half maximum (FWHM) line width. This was not possible for features detected in fewer than three channels (indicated by a missing line width in Table 1), so the peak flux and center velocity of the channel of the brightest maser emission are given for these features instead. Taking into account the flux scale caveat, the brightest 6035 MHz maser in ON 1 is approximately as bright or brighter than any maser seen in the ground-state transitions (Fish et al. 2005a; Nammahachak et al. 2006; Fish & Reid 2007), as noted in W3(OH) as well (Fish et al. 2006a; Fish & Sjouwerman 2007).

The locations of the masers are shown in Figure 1. Also shown are ground-state masers detected with the Multi-Element Radio Linked Interferometer Network (MERLIN) by Nammahachak et al. (2006) and with the Very Long Baseline Array (VLBA) by Fish & Reid (2007). The Fish & Reid (2007) data are aligned relative to the Nammahachak et al. (2006) data using the brightest maser detected in the former. The 6035 MHz masers appear to have a similar distribution to the ground-state masers near the continuum region. The apparent systematic southward-eastward shift of the 6035 MHz masers relative to the ground-state masers is significantly less than the beam size and is within the error of determining the relative alignment between the 6035 MHz and continuum reference frames.

Position centroids of the masers as measured in consecutive channels differ at the  $0''.2$  level but do not shift systematically with LSR velocity. This could be due to blending of nearby maser spots at slightly different velocities or due to position uncertainties caused by the sparse  $uv$ -coverage and consequent beam elongation. The relative uncertainty in position accuracy between RCP and LCP spots is negligible ( $< 0''.01$ ) in comparison. Future observations with the EVLA, when more antennas with extended C-band tuning capability are available, should provide much better image fidelity, with correspondingly better determination of maser positions.

The 6035 MHz maser velocities are systematically offset by approximately  $0.1 \text{ km s}^{-1}$  from the Baudry et al. (1997) Effelsberg observations,  $0.2 \text{ km s}^{-1}$  from the Fish et al. (2006b) Effelsberg observations, and  $0.3 \text{ km s}^{-1}$  from the EVN observations of Desmurs & Baudry (1998). Accounting for this, masers appear to be brighter on average than in previous epochs; for instance, the brightest maser is at least three times as bright as seen by Baudry et al. (1997) and Fish et al. (2006b). The overall brightening exceeds the errors due to the uncertain flux scale calibration in these observations and therefore appears to be a real effect.

#### 3.2. Magnetic Fields

Based on positional coincidence (within the 200 mas uncertainties) of LCP and RCP maser features at statistically significant different LSR velocities, six Zeeman pairs are detected at 6035 MHz, listed in Table 2 and indicated in red on Figure 1. This gives 5 unambiguous pairs as well as a sixth ambiguous pair, as noted in Table 2, all consistently indicating a negative magnetic field (i.e., one whose line-of-sight projection points toward the observer). Three pairs where the velocity difference is less than the uncertainties are not included; these could be due to small magnetic fields, linear polarization, or the pairing of unrelated features. Assuming that the 6035 MHz masers should be shifted northward and westward slightly, the  $-4.8 \text{ mG}$  magnetic field agrees with the magnetic field values obtained at 1665 MHz. This also agrees with a previous Zeeman measurement of this 6035 MHz pair of  $-5.3 \text{ mG}$  by Desmurs & Baudry (1998), correcting for the previously noted velocity offsets. Magnetic fields of approximately  $-5 \text{ mG}$  are detected on the western side of the continuum emission, in contrast with a weaker  $-1.9 \text{ mG}$  field detected at 1665 MHz. The 6030 MHz  $-4.8 \text{ mG}$  Zeeman pair detected by Fish et al. (2006b) may be located near the 6035 MHz  $-5.7 \text{ mG}$  Zeeman pair at the same corrected systemic velocity, since Fish & Sjouwerman (2007) note that 6030 MHz masers have a strong tendency to appear in very close spatial coincidence with brighter 6035 MHz masers. In any case, the magnetic field as detected by OH masers appears to be negative throughout the source, although the data do not rule out line-of-sight field reversals on small scales or where no masers are detected.

In the north, large ( $\sim -10 \text{ mG}$ ) magnetic fields are detected. Due to the large number of maser features in the north, single-dish measurements have had difficulty pairing the maser features unambiguously to determine a magnetic field. Baudry et al. (1997) claim a magnetic field of  $-2.7 \text{ mG}$ , while Fish et al. (2006b) claim magnetic fields from  $-5.2$  to  $-12.8 \text{ mG}$  at blueshifted velocities in the 6035 MHz transition, as well as a  $-13.5 \text{ mG}$  Zeeman pair at 6030 MHz, whose systemic velocity is consistent with the 6035 MHz  $-12.1 \text{ mG}$  Zeeman pair in Table 2, when correcting for the  $0.2 \text{ km s}^{-1}$  offset. The larger (absolute) values are also more consistent with the  $-8.3 \text{ mG}$  Zeeman pair detected in the blueshifted masers in the 13441 MHz highly excited state (Fish et al. 2005b). Future observations at higher angular and spectral resolution may be useful to confirm and reduce the errors on measurements of the magnetic field values at 6035 MHz.

The ratio of the fluxes of the bright to weak components of a Zeeman pair ranges from  $\gtrsim 1.0$  to 2.1 at 6035 MHz. The equivalent ratio for 1665 MHz masers is 2.1–34.4, while at 1667 MHz two Zeeman pairs have flux ratios of 2.3 and 2.8 (Fish & Reid 2007). The two 1720 MHz Zeeman pairs detected by Nammahachak et al. (2006) each have a flux ratio of 1.1. The Zeeman pairs in ON 1 thus fit the general pattern that the flux ratio between Zeeman components decreases with decreasing Zeeman splitting coefficient (0.59, 0.354, 0.114<sup>1</sup>, and 0.0564  $\text{km s}^{-1} \text{ mG}^{-1}$  at 1665, 1667, 1720, and 6035 MHz, respectively; Davies 1974).

### 4. DISCUSSION

#### 4.1. Environment of the Masers in ON 1

<sup>1</sup> Davies (1974) and Nammahachak et al. (2006) assume a splitting twice this at 1720 MHz, appropriate for blending of multiple  $\sigma$  components, but a detailed study of the 1720 MHz line profiles in another source, W3(OH), failed to find evidence of the outer hyperfine lines (Fish et al. 2006a).

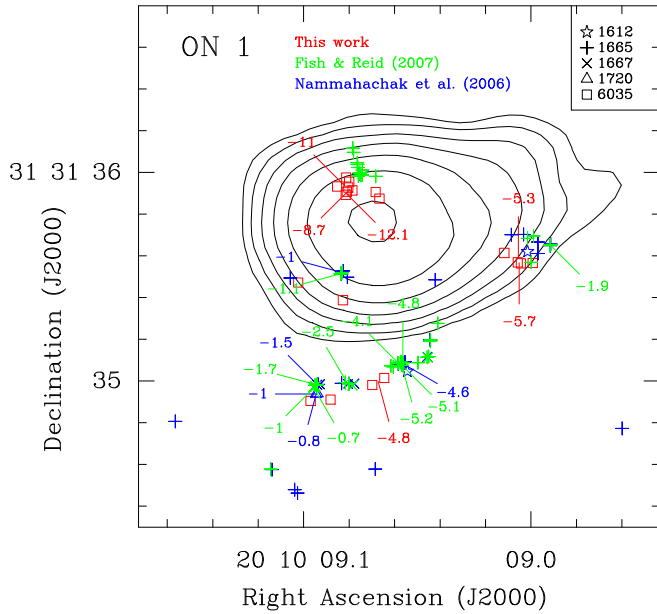


FIG. 1.— Map of maser emission in ON 1. Contours indicate 8.4 GHz continuum emission from the Argon et al. (2000) data. Ground-state masers detected by Nammahachak et al. (2006) and Fish & Reid (2007) are shown in blue and green respectively, while 6035 MHz masers (this work) are shown in red. Numbers indicate magnetic fields in milligauss obtained from Zeeman splitting at the location pointed to by the associated line, color-coded by source. The small apparent southeastward shift of the 6035 MHz masers relative to other maser transitions is not significant.

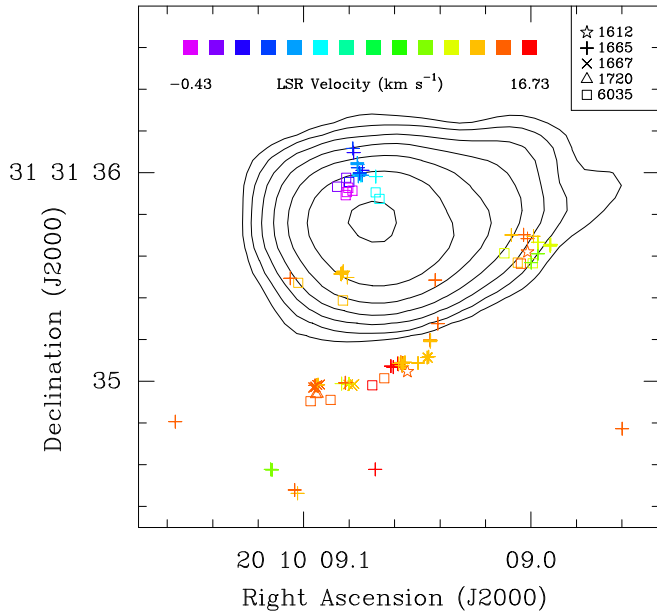


FIG. 2.— Velocity map of maser spots. The LSR velocities of maser spots from this work, Nammahachak et al. (2006), and Fish & Reid (2007) are indicated in color. Northern masers are highly blueshifted compared to masers in the south. Velocities are not corrected for Zeeman splitting, which can be significant at 1665 and 1667 MHz.

The distributions of the 1665 and 6035 MHz masers are the most alike of any pair of OH transitions in ON 1. All the 1665 MHz maser regions have associated 6035 MHz masers, apart from in the center and in the extreme south, far from the exciting source where densities are likely to be low. The brightest masers at both transitions occur in the line of maser spots just south of center in Figure 1. This contrasts with

TABLE 1  
DETECTED MASERS AT 6035 MHz

Pol.	$v_{\text{LSR}}$ ( $\text{km s}^{-1}$ )	R.A. Offset (mas)	Decl. Offset (mas)	Peak Brightness ( $\text{Jy beam}^{-1}$ )	$\Delta v$ ( $\text{km s}^{-1}$ )	Zeeman Pair
LCP	$0.06 \pm 0.03$	-105	1003	1.10	0.29	1
	$0.69 \pm 0.03$	-78	996	2.73	0.28	2
	$1.39 \pm 0.08$	-75	1065	0.20	...	...
	$2.31 \pm 0.03$	-89	1045	0.76	0.25	3
	$5.79 \pm 0.08$	-234	964	0.50	...	...
	$12.76 \pm 0.08$	-833	703	0.38	...	4
	$13.96 \pm 0.02$	155	561	2.74	0.32	...
	$14.29 \pm 0.02$	-912	653	3.67	0.36	5
	$14.70 \pm 0.02$	96	-6	7.83	0.24	...
	$15.65 \pm 0.02$	-200	70	3.48	0.25	6
RCP	$-0.43 \pm 0.08$	-85	1017	1.98	...	1
	$0.01 \pm 0.02$	-72	982	5.72	0.26	2
	$1.69 \pm 0.08$	-31	1022	0.40	...	3
	$5.72 \pm 0.02$	-216	995	2.96	0.27	...
	$12.46 \pm 0.08$	-969	655	0.40	...	4
	$13.97 \pm 0.08$	-59	477	6.17	...	...
	$13.97 \pm 0.08$	-897	658	6.10	...	5
	$14.69 \pm 0.01$	0	0	49.47	0.20	...
	$15.38 \pm 0.01$	-257	104	4.57	0.27	6

NOTE. — Reference feature location is  $20^{\text{h}}10^{\text{m}}09^{\text{s}}.090$ ,  $+31^{\circ}31'34''.91 \pm 0''.2$  (J2000). Line widths are FWHM. Zeeman pairs are listed in Table 2

TABLE 2  
ZEEMAN PAIRS AT 6035 MHz

Pair Number	$v_{\text{LSR}}^a$ ( $\text{km s}^{-1}$ )	$B$ (mG)
1	$-0.18 \pm 0.08$	$-8.7 \pm 1.4$
2	$0.35 \pm 0.04$	$-12.1 \pm 0.7$
3	$2.00 \pm 0.08$	$-11.0 \pm 1.4^b$
4	$12.61 \pm 0.11$	$-5.3 \pm 1.9$
5	$14.13 \pm 0.08$	$-5.7 \pm 1.4$
6	$15.52 \pm 0.02$	$-4.8 \pm 0.4$

<sup>a</sup> Systemic velocity:  $0.5 * (v_{\text{LCP}} + v_{\text{RCP}})$ .

<sup>b</sup> While the RCP feature could pair with LCP  $1.39 \text{ km s}^{-1}$ , this would give a magnetic field of  $+5.3 \text{ mG}$ , inconsistent in sign and magnitude with other features in the region.

the 1612, 1667, and 1720 MHz masers, which are only found in the prominent line of masers south of and on the southwestern limb of the continuum source. A similar result was seen at VLBI resolution in W3(OH): 1665 and 6035 MHz masers appear throughout the source, 1612 and 1720 MHz masers appear only in and near the inner edge of an apparent shocked torus that is especially well traced by 6.0 GHz masers (including several of the brightest 6.0 GHz masers detected), and 1667 MHz emission is largely concentrated in areas with an apparent shock morphology (Fish & Sjouwerman 2007). Higher-resolution observations of the 6.0 GHz masers in ON 1 would be useful to obtain a better alignment of the 6035 MHz frame with respect to the other masers and determine whether the southern masers are located preferentially along the northern edge of the southern shock front.

Some of the 6035 MHz masers may be associated with an outflow, such as the  $\text{H}^{13}\text{CO}^+$  oriented northeast-southwest through ON 1 detected by Kumar et al. (2004). Nammahachak et al. (2006) note that the southern line of OH masers is oriented nearly perpendicular to this structure and propose, based additionally on the linear polarization characteristics of the ground-state masers, that the masers trace a shock in a confining molecular torus. Sim-

ilar conclusions based on maser distribution and polarization are reached for other OH maser sources hosting outflows (Hutwarakorn & Cohen 1999, 2003, 2005; Hutwarakorn et al. 2002). This interpretation also bears a striking similarity to that proposed for W3(OH), which hosts very strong 6035 MHz masers (Fish & Sjouwerman 2007), and may therefore suggest a common mechanism for producing strong 6035 MHz maser emission.

It is probable that there is a coherent, organized structure in the northern part of ON 1. Many LCP 1665 MHz masers, including one bright one, occur in the region, with a few weak RCP masers offset to the north and west of the LCP emission (Fish et al. 2005a; Fish & Reid 2007). Assuming a magnetic field of approximately  $-10$  mG in the region, LCP and RCP 1665 MHz maser components would be separated by  $6 \text{ km s}^{-1}$  ( $20 \Delta v$  for an average line width of  $0.3 \text{ km s}^{-1}$ ) if they both appear in the region. (It is likely that weak RCP 1665 MHz masers, seen near  $-2 \text{ km s}^{-1}$  in the spectra of Clegg & Cordes (1991), pair with the dominant LCP masers near  $+4 \text{ km s}^{-1}$ , but no published interferometric observations of the ground-state masers have included the  $-2 \text{ km s}^{-1}$  features in the observed bandpass.) If the magnetic field and velocity gradients are aligned such that the magnetic field strength decreases (becomes less negative) in the same direction that the velocity increases, amplification of the LCP component would be favored (see Cook 1966). This effect is much more pronounced for ground-state OH masers than at 6035 MHz, where the Zeeman splitting is a factor of 10 smaller in velocity units, such that the LCP and RCP spectra are separated by  $0.6 \text{ km s}^{-1} \approx 2 \Delta v$  per 10 mG, which is not in excess of the turbulent velocity component expected in a maser condensation (Reid et al. 1980). Hence, 6035 MHz masers appear in both polarizations with similar fluxes, while strong LCP 1665 MHz emission appears at higher velocities (and possibly weaker RCP emission at lower velocities).

The key question that remains is how the blueshifted masers in the north connect to the redshifted masers in the south. It is tempting to associate both with the  $\text{HCO}^+$  outflow, but the northern masers are significantly blueshifted compared to the  $\text{HCO}^+$  velocity range of  $8\text{--}16 \text{ km s}^{-1}$  (Kumar et al. 2004). These authors also note a CO outflow in the region that spans a larger velocity range, but it is oriented roughly east-west. Kumar et al. (2004) interpret the outflows as coming from two different sources embedded in the ultracompact H II region. It is possible that the blue and red OH masers are also associated with two different sources, which would complicate interpretation of their motions and morphology. The large ( $|B| > 10$  mG) magnetic fields suggest that the northern masers are near a region of higher density and therefore

likely an excitation source. In W3(OH) the methanol masers in the region of highest magnetic field strength ( $|B| > 10$  mG) have been modelled as undergoing conical expansion, which Moscadelli et al. (2002) interpret as possibly being due to an outflow guided by the helical field from a magnetized disk.

#### 4.2. Future Directions

Excluding minor transitional issues, the performance of the EVLA antennas was as expected. Early data from the antennas with upgraded C-band capability are of good quality and are already producing useful science (e.g., Sjouwerman et al. 2007). As the upgrade continues, more antennas with 6.0 GHz tuning capability will be added to the array, providing proportionally better sensitivity and imaging characteristics.

High spectral resolution VLBI observations of the 1665 and 6035 MHz OH masers, of the sort obtained for W3(OH) (Fish et al. 2006a; Fish & Sjouwerman 2007), may help answer the questions of whether there is an organized velocity structure in the north and what structure the masers are tracing. If the segregated regions of LCP and RCP emission in the north are due to correlated magnetic and velocity field gradients, small-scale velocity gradients (i.e., on the size scale of a maser spot) of the northern masers may show similar magnitudes and position angles. This would contrast with W3(OH), in which small-scale velocity gradients show no correlation except when masers overlap (Fish et al. 2006a; Fish & Sjouwerman 2007). Any such observations of the ground-state masers should have a sufficiently wide bandwidth coverage to include the  $-2 \text{ km s}^{-1}$  1665 MHz masers in order to be able to identify magnetic field strengths (and variations thereof) throughout the northern masers. While observations of linear polarization exist for the ground-state masers (Nammahachak et al. 2006), full-polarization observations at 6035 MHz would help to understand the magnetic field geometry, since linear polarization vectors are much less subject to being corrupted by external and internal Faraday rotation at the higher frequency (e.g., Fish & Reid 2006).

The National Radio Astronomy Observatory is a facility of the National Science Foundation operated under cooperative agreement by Associated Universities, Inc. The VLA Calibrator Manual can be found at <http://www.vla.nrao.edu/astro/calib/manual/csources> and the VLA flux density history database can be accessed at <http://aips2.nrao.edu/vla/calflux.html>. The author wishes to acknowledge helpful comments from L. O. Sjouwerman in the manuscript preparation phase.

*Facilities: EVLA*

#### REFERENCES

- Argon, A. L., Reid, M. J., & Menten, K. M. 2000, *ApJS*, 129, 159  
 Baudry, A., Desmurs, J. F., Wilson, T. L., & Cohen, R. J. 1997, *A&A*, 325, 255  
 Clegg, A. W., & Cordes, J. M. 1991, *ApJ*, 374, 150  
 Cook, A. H. 1966, *Nature*, 211, 503  
 Davies, R. D. 1974, *Galactic Radio Astronomy*, 60, 275  
 Desmurs, J. F., & Baudry, A. 1998, *A&A*, 340, 521  
 Fish, V. L., Brisken, W. F., & Sjouwerman, L. O. 2006a, *ApJ*, 647, 418  
 Fish, V. L., & Reid, M. J. 2006, *ApJS*, 164, 99  
 Fish, V. L., & Reid, M. J. 2007, *ApJ*, in press, arXiv:0708.1186  
 Fish, V. L., Reid, M. J., Argon, A. L., & Zheng, X.-W. 2005a, *ApJS*, 160, 220  
 Fish, V. L., Reid, M. J., & Menten, K. M. 2005b, *ApJ*, 623, 269  
 Fish, V. L., Reid, M. J., Menten, K. M., & Pillai, T. 2006b, *A&A*, 458, 485  
 Fish, V. L., & Sjouwerman, L. O. 2007, *ApJ*, in press, arXiv:0706.3352  
 Ho, P. T. P., Haschick, A. D., Vogel, S. N., & Wright, M. C. H. 1983, *ApJ*, 265, 295  
 Hutwarakorn, B., & Cohen, R. J. 1999, *MNRAS*, 303, 845  
 Hutwarakorn, B., & Cohen, R. J. 2003, *MNRAS*, 343, 175  
 Hutwarakorn, B., & Cohen, R. J. 2005, *MNRAS*, 357, 338  
 Hutwarakorn, B., Cohen, R. J., & Brebner, G. C. 2002, *MNRAS*, 330, 349  
 Kumar, M. S. N., Tafalla, M., & Bachiller, R. 2004, *A&A*, 426, 195  
 McKinnon, M., & Perley, R. (Eds.) 2001, "The VLA Expansion Project", <http://www.aoc.nrao.edu/evla/pbook.shtml>  
 Moscadelli, L., Menten, K. M., Walmsley, C. M., & Reid, M. J. 2002, *ApJ*, 564, 813  
 Nammahachak, S., Asanok, K., Hutwarakorn Kramer, B., Cohen, R. J., Muanwong, O., & Gasiprongs, N. 2006, *MNRAS*, 371, 619

- Reid, M. J., Haschick, A. D., Burke, B. F., Moran, J. M., Johnston, K. J., & Swenson, G. W. Jr. 1980, *ApJ*, 239, 89
- Sjouwerman, L. O., Fish, V. L., Claussen, M. J., Pihlström, Y. M., & Zschaechner, L. K. 2007, *ApJL*, in press, arXiv:0707.3788
- Szymczak, M., Hrynek, G., & Hus, A. J. 2000, *A&AS*, 143, 269
- Ulvestad, J. S., Perley, R. A., McKinnon, M. M., Owen, F. N., Dewdney, P. E., & Rodriguez, L. F. 2006, *BAAS*, 38, 135
- Zheng, X. W., Ho, P. T. P., Reid, M. J., & Schneps, M. H. 1985, *ApJ*, 293, 522